Recent Results on Top Quark Physics and B Physics at CDF

Shinhong Kim
(for the CDF Collaboration)
University of Tsukuba, Tsukuba, Ibaraki, 305, Japan

Abstract

We present the recent results on top quark physics and B physics with the Collider Detector at Fermilab (CDF). These results come from analyses using a full data sample at an integrated luminosity of 109 pb^{-1}. We describe the measurements of the top quark mass and the $t\bar{t}$ production cross section in 1.8-TeV $p\bar{p}$ collisions. We measure the top quark mass to be 175.9±6.9 GeV/c^2 and the $t\bar{t}$ production cross section to be $7.6^{+1.8}_{-1.5}$ pb. We also present the measurements of the lifetimes of B-hadrons and the time-dependent $B^0 - \bar{B}^0$ mixing which results in the mass difference between heavy and light B_d^0 mesons (Δm_d) of 0.464±0.030(stat)±0.026(syst) ps^{-1}.

1 Introduction

In Tevatron Run1 (1992-1995), we collected the data corresponding to an integrated luminosity of 109±7 pb^{-1}, and we had over 5×10^{12} $p\bar{p}$ collisions. About 500 top quark pairs and 10^9 bottom quark pairs were produced in Run1. Since these numbers of pairs are the highest in the world, a Tevatron collider experiment is a good place to study top quark physics and B physics.

Since a discovery of a bottom quark in 1977 [1], a top quark which is a weak-isospin partner of the bottom quark has been searched for at various collider experiments. In April 1994, the CDF collaboration reported the first evidence for top quark production [2] where 15 $t\bar{t}$ candidates events were found against 6.0 background events expected. It corresponded to 2.8σ excess. CDF measured the top quark mass M_{top} to be 174±17 GeV/c^2 and the $t\bar{t}$ production cross section $\sigma_{t\bar{t}}$ to be $13.9^{+6.1}_{-4.8}$ pb. In February 1995, the CDF and D0 confirmed the existence of top quark production [3, 4]. The CDF reported that $t\bar{t}$ signals had 4.8σ excess, M_{top}=176±8(stat)±10(syst) GeV/c^2 and $\sigma_{t\bar{t}} = 6.8^{+3.6}_{-2.4}$ pb. The D0 reported that $t\bar{t}$ signals had 4.6 σ excess, $M_{top} = 199^{+19}_{-21}$(stat)$^{+14}_{-21}$(syst) GeV/c^2 and $\sigma_{t\bar{t}} = 6.4 \pm 2.2$ pb. We will present the measurements of the top quark mass and the $t\bar{t}$ production cross section and the search for top quark rare decays with a full data sample in Run1.

In Run1, we collected a signal of 243,000 J/ψ, from which we reconstructed a signal of fully reconstructed decays of about 1,000 $B \to J/\Psi K$ and 58±12 $B_s \to J/\Psi\phi$. In addition, we extracted a signal of 6,000 partially reconstructed decays $B \to D(D^*)\ell\nu X$. These signals were obtained after requiring that the charged decay products be in the acceptance of the silicon vertex detector. This fiducial requirement reduces the signals by approximately a factor of two, but allows a precision lifetime measurement as well as a significant reduction of combinatoric background. Based on these signals, we have studied the masses and lifetimes of B-hadrons. Here we present the measurements of the lifetimes of B-hadrons and time-dependent $B^0 - \bar{B}^0$ mixing, which measures the mass difference between heavy and light B_d^0 mesons (Δm_d).

2 The CDF detector

The CDF detector consists of a magnetic spectrometer surrounded by calorimeters and muon chambers [5]. A silicon vertex detector (SVX), located immediately outside the beampipe, provides precise track reconstruction in the plane transverse to the beam and is used to identify secondary vertices from b and c quark decays [6]. The momenta of charged particles are measured in the central tracking chamber (CTC) which is in a 1.4 T superconducting solenoidal magnet. Outside the CTC, electromagnetic and hadronic calorimeters cover the pseudorapidity [7] region $|\eta| < 4.2$ and are used to identify jets and electron candidates. Outside the calorimeters, drift chambers in the region $|\eta| < 1.0$ provide muon identification.

3 Top Quark Physics

Within the standard model, the top quark decays predominantly to Wb. We categorize the decays of $t\bar{t}$ pairs into the following three channels by the decay of the two W bosons:

- Dilepton channel: Both W bosons decay leptonically. The final state is $l^+\nu l^-\nu b\bar{b}$ ($l = e$ or μ; BR = 5%).
- Lepton+jets channel: One W decays hadronically and another decays leptonically. The final state is $l^+\nu q\bar{q}^{'} b\bar{b}$ ($l = e$ or μ; BR = 30%).
- All-hadronic channel: Both W bosons decay hadronically. The final state is $q\bar{q}^{'} q\bar{q}^{'} b\bar{b}$ (BR = 44%)

In the dilepton channel, we require two high P_T lepton (e or μ) with $P_T > 20$ GeV/c, high missing transverse energy ($\not{E}_{\rm T} > 25$ GeV) to account for the presence of two undetected neutrinos and two jets with $E_T > 10$ GeV and $|\eta| < 2.0$. In the all-hadronic channel, we search for the events with five or more jets ($E_T > 15$ GeV and $|\eta| < 2.0$), requiring at least one b-jet identified with the SVX tagging algorithm described later as well as topological cuts to reduce the very large QCD backgrounds. In the lepton+jets channel, we require one isolated high P_T lepton (e or μ) with $P_T > 20$ GeV/c, high missing transverse energy ($\not{E}_{\rm T} > 20$ GeV) from a neutrino and 3 or more jets with $E_T > 15$ GeV in $|\eta| < 2.0$.

In this paper, we mainly describe the analyses in the lepton+jets channel. Dominant background is $p\bar{p} \to W(\to l\nu)$+jets. In order to separate $t\bar{t}$ events in the lepton+jets channel from the large W+jets background, we require that one of the jets be identified as a b-quark jet. We tag b-jets by reconstructing displaced vertices from b-quark decay using the SVX (SVX tagging), or identifying an additional lepton from a semileptonic b decay (SLT tagging). Details of the SVX and SLT tagging algorithms are described in Ref. [3].

3.1 $t\bar{t}$ Production Cross Section

We measure the $t\bar{t}$ production cross section [8] which tests both the production and decay mechanisms of the standard model. Recent calculations based on Quantum Chromodynamics (QCD) [9] have led to predictions for the cross section from 4.8 to 5.5 pb at a top quark mass of 175 GeV/c^2 with a theoretical uncertainty of less than 15%.

The efficiency for tagging a b quark from a top decay is determined from $t\bar{t}$ Monte Carlo data together with a detailed simulation of the detector, which includes the effect of local track density on the tracking efficiency. The systematic uncertainty due to the tracking efficiency modeling is determined by comparing the Monte Carlo tracking efficiency with that in the inclusive lepton(e or μ) data which are enriched in b-decay. The efficiency for tagging at least one b quark in a $t\bar{t}$ event with $\geq$3 jets using the SVX algorithm is found to be (39$\pm$3)%. Of the 39%, a factor of 67% comes from the fiducial acceptance of the SVX. The SLT algorithm identifies both muons and electrons with $P_T > 2.0$ GeV/c in $|\eta| < 1.0$. The probability of finding an additional e or μ from a b quark decay in a $t\bar{t}$ event with $\geq$3 jets is (18$\pm$2)%.

In the $t\bar{t}$ signal region of $W+\geq$ 3jets, there are 34 SVX-tagged events containing a total of 42 SVX tags, and 40 SLT-tagged events containing a total of 44 SLT tags. Of these, 11 events are tagged by both the SVX and SLT algorithms.

The acceptance for identifying $t\bar{t}$ events in the lepton+jets channel is calculated from a combination of data and $t\bar{t}$ Monte Carlo samples at a top quark mass of 175 GeV/c^2. The total acceptance, including the branching fraction, is calculated as the product of the kinematic (including lepton identification) and geometric acceptances, the trigger efficiency and the tagging efficiency. Measuring these efficiencies as described in Ref. [2], we obtain the product of the geometric and kinematic acceptance of (10.4$\pm$1.0)% and the trigger efficiency of (90$\pm$7)%. Combining with the respective tagging efficiencies gives a total SVX acceptance of (3.4$\pm$0.5)% and a total SLT acceptance of (1.7$\pm$0.3)%.

The most important source of backgrounds in the b-tagged lepton+jets channel is inclusive W production in association with jets containing b or c quarks, e.g. $p\bar{p} \to Wg(g \to b\bar{b})$. In addition, there are contributions to the background from mistags which are tags in non-b jets, and small contributions from the following processes: non-W(e.g. direct $b\bar{b}$ production), single top production, WW, WZ, and Drell-Yan.

To calculate the background from W+heavy flavor events, we use HERWIG [10] and VECBOS [11] Monte Carlo programs to predict the fraction of W+jets events which are $Wb\bar{b}$, $Wc\bar{c}$ and Wc as a function of jet multiplicity. These fraction are applied to the number of W+jet events seen in the data to give an expected background from these sources for each jet multiplicity. The details of this method can be found in Ref. [2].

Thus we have 34 SVX-tagged (40 SLT-tagged) events with an expected background of 9.2 (22.6) events as listed in Table 1.

$b \to lX$	
Observed	40 events (44 tags)
Background	22.6 $\pm$ 2.8
Expected $t\bar{t}$ Yield (M_{top}=175 GeV/c^2)	14.3 $\pm$ 2.7
Displaced Vertex	
Observed	34 events (42 tags)
Background	9.2 $\pm$ 1.5
Expected $t\bar{t}$ Yield (M_{top}=175 GeV/c^2)	31.0 $\pm$5.9

Table 1: Summary of event yields from the lepton+jets analyses. The expected $t\bar{t}$ yields are calculated using the measured cross section from this paper.

Our best measurement of the $t\bar{t}$ production cross section comes from combining the results of the lepton+jets analyses with the dilepton and all-hadronic analyses [12, 13]. The results of the individual analyses are summarized in Table 2. The dilepton analysis finds 9 candidate events, with an expected background of 2.4$\pm$0.5 events. The all-hadronic analysis has two parallel paths, one with a single SVX tagged jet plus kinematic cuts and another with only two SVX tagged jets. We have 187 candidates events with an expected background of 142$\pm$12 events in single SVX tag sample, and 157 candidates events with an expected background of 120$\pm$18 events in double SVX tag sample. There are 34 candidates events in common between the two samples. The dilepton, lepton+jets and all-hadronic data samples are exclusive sets.

	Lepton+jets		Dilepton	All-hadronic	
Tag	SVX	SLT	not req.	SVX	2SVX
ϵ_{total}	0.037$\pm$0.005	0.017$\pm$0.003	0.0074$\pm$0.0008	0.044$\pm$0.010	0.030$\pm$0.010
Observed	34	40	9	187	157
Background	9.2$\pm$1.5	22.6$\pm$2.8	2.4$\pm$0.5	142$\pm$12	120$\pm$18
$\sigma_{t\bar{t}}$(pb)	$6.2^{+2.1}_{-1.7}$	$9.2^{+4.3}_{-3.6}$	$8.2^{+4.4}_{-3.4}$	$9.6^{+4.4}_{-3.6}$	$11.5^{+7.7}_{-7.7}$

Table 2: Summary of total efficiency and measured cross section for each analysis channel. The acceptances are calculated for a top quark mass of 175 GeV/c^2.

We calculate the $t\bar{t}$ production cross section to be $7.6^{+1.8}_{-1.5}$ pb by combining the results in the dilepton, lepton+jet and all-hadronic channels, where the quoted uncertainty includes both statistical ($\pm$1.2 pb) and systematic uncertainties. This result is a little higher than the theoretical prediction but consistent with it within the uncertainties on the measurement and the theory.

3.2 Top Quark Mass

A top quark mass is a fundamental parameter of the standard model. We report the measurement of the top quark mass in the lepton+jets channel [14]. We require an additional jet with $E_T > 8$ GeV and $|\eta| < 2.4$ in the $W+ \geq 3$ jet event sample to make a $W+ \geq 4$ jet sample for the top quark mass analysis.

At first we perform an event fitting: In the sample of $W+ \geq 4$ jet events, we can make a one-to-one mapping of jets to quarks (using the 4 highest E_T jets) assuming the decay chain:

$$\begin{aligned} p\bar{p} &\to t_1 + t_2 + X \\ t_1 &\to b_1 + W_1 \\ t_2 &\to b_2 + W_2 \\ W_1 &\to \ell + \nu \\ W_2 &\to j_1 + j_2 \end{aligned}$$

There are 24 combinations with which to try. We impose $M_{t1} = M_{t2}$ and $m(j_1 j_2) = m(\ell\nu) = M_W$, the measured W mass. Energy and momentum conservation plus these constraints give 20 equations with 18 unknowns which results in a 2-C constrained fit. This fit is performed by a standard χ^2-minimization technique. As a b-tagged jet is only used as a b, there are 12 possible combinations with 1 b tag and 4 combinations with 2 b tags. In this event fitting, we choose only one specific combination with the lowest χ^2. The output of each event fit is a reconstructed top mass M_{rec} and a χ^2 value quantifying how well the event is described by the $t\bar{t}$ hypothesis.

Next we use a likelihood method to extract a measured top mass from a sample of $t\bar{t}$ candidates. We fit the M_{rec} distributions for the $t\bar{t}$ candidate events to a sum of those for the Monte Carlo $t\bar{t}$ signal and backgrounds which we call templates. The $t\bar{t}$ signal template f_s is adequately represented by a sum of two components, a Gaussian which describes mainly events where all parton-jet assignments are correctly reconstructed, and a gamma distribution for the remaining events for a fixed top mass M_{top}:

$$f_s(M_{rec}, M_{top}) = \frac{1-P_6}{\sqrt{2\pi}P_5} e^{-\frac{1}{2}(\frac{M_{rec}-P_4}{P_5})^2} + \frac{P_6 P_3^{(1+P_2)}}{\Gamma(1+P_2)} (M_{rec} - P_1)^{P_2} e^{-P_3(M_{rec}-P_1)}$$

The parameters of the Gaussian and gamma distributions are themselves linear functions of M_{top}: $P_i = \alpha_i + \alpha_{i+6} M_{top}$. In all, twelve parameters α_j are needed. They are determined by a simultaneous fit to eighteen reconstructed mass distributions corresponding to input top mass ranging from 120 to 220 GeV/c^2 calculated with the HERWIG program. The background template f_b is represented by a gamma distribution except for the untagged event sample where the background template is represented by a sum of a Gaussian and a gamma distribution. This shape f_b is determined by fitting a gamma distribution (or a sum of a Gaussian and a gamma distribution) to a reconstructed mass distribution generated with the VECBOS W+jets Monte Carlo program. We make a likelihood function by the sum of the signal and background templates. By maximizing this likelihood with respect to M_{top}, a background fraction and the template parameters, we measure M_{top} and $\sigma_{M_{Top}}$.

The precision of the top quark mass measurement is expected to increase with the number of observed events, the signal-over-background ratio, and the naturalness of the reconstructed-mass distribution. These characteristics vary significantly between samples with different b tagging requirements. Therefore, to make optimal use of all the available information, we partition the top mass sample into non-overlapping subsamples. Monte carlo studies showed that a good partition is made up of four subsamples: events with a single SVX tag, events with two SVX tags, events with an SLT tag but no SVX tag, and events with no tag, but with the tighter kinematic requirement of four jets with $E_T \geq 15$ GeV and $|\eta| \leq 2$.

We measure the top quark mass to be 175.9$\pm$4.8(stat)$\pm$4.9(syst) GeV/c^2 as shown in Fig. 1. Systematic uncertainties on the top quark mass are listed in Table 3. The largest one comes from the jet energy measurement. The jet energy corrections carry an energy-dependent uncertainty. For an observed jet E_T of 40 GeV, the total uncertainty on the corrected E_T varies between 3.4 and 5.6% depending on the proximity of the jet to cracks between detector components.

Summarizing the top quark mass analysis, we obtain new precise results with the optimal use of the information. The CDF top quark mass is M_{top} = 175.9$\pm$6.9 GeV/c^2 in the lepton+jets channel. A top quark mass together with a W mass yields a constraint to a Higgs mass as shown in Fig. 2. The present

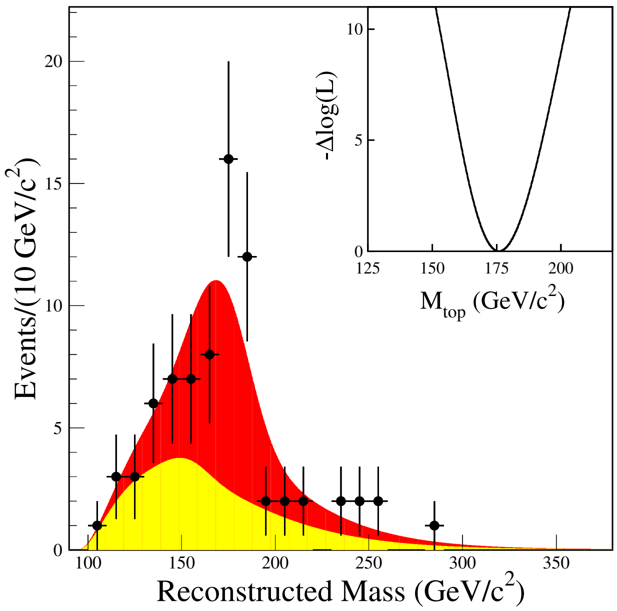

Figure 1: The reconstructed-mass distribution of the four top mass samples combined. The data (points) are compared with the result of the combined fit (dark shading), and with the background component of the fit (light shading). The inset shows the variation of the combined negative log-likelihood with top quark mass.

allowed Higgs mass is 115^{+116}_{-66} GeV/c^2 and less than 430 GeV/c^2 at 95% confidence level [15] from the CDF results combined with D0 results and a LEP W mass.

3.3 Hadronic W decays in $W+\geq 4$ jet events

In the above lepton+jet analyses, we assume that one W decays hadronically into $q\bar{q}'$. In order to confirm that this assumption is right, we need present that hadronic W decays exist in $W+\geq 4$ jet events which is consistent with the expectation from $t\bar{t}$ signals.

We search the second W decaying hadronically as a dijet invariant mass peak in the lepton+jets channel applying either of the following two selection criteria [16]:

- $H_T > 310$ GeV cut, where H_T is a scalar sum of parton P_T's (H_T cut sample).
- requiring two b-tagged jets (two b-tagged sample).

CDF L+Jet Mass Systematic	Value GeV/c^2
Jet energy measurement	4.4
Initial and final state radiation	1.8
shape of background spectrum	1.3
b tag bias	0.4
Parton distribution function	0.3
Total	4.9

Table 3: Systematic uncertainties on top quark mass.

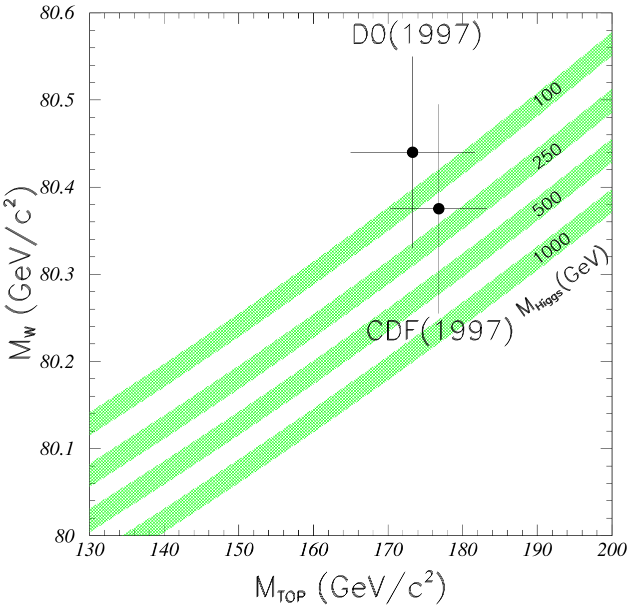

Figure 2: W mass versus top quark mass. Prediction curves are shown for various Higgs masses.

We observe a W mass peak with a significance of 2.8σ in the H_T cut sample and of 2.9σ in the two b-tagged sample as shown in Fig. 3. Combining these two results, we obtain the W mass peak significance of 3.3σ ($Prob = 5.4 \times 10^{-4}$). The measured W mass is 77.2±3.5(stat)±2.9(syst) GeV/c^2. This is consistent with the current world-average W mass of 80.375±0.120 GeV/c^2 [17].

Top mass analysis is the first measurement of a new particle mass using jet four momenta. Top mass measurement together with this hadronic W decay observation presents that we can use the jet four momenta as the quark/gluon four momenta for new particle searches.

3.4 Measurement of V_{tb}

Unitarity within a three-generation standard model implies V_{tb} is almost 1.0. We have analyzed the lepton+jets and dilepton samples to measure the ratio of events with 0, 1, and 2 b-tags and extract $b = BR(t \to Wb)/BR(t \to WX)$. By comparing ratios of these event yields, this result is independent of the values of $\sigma_{t\bar{t}}$ and $BR(W \to l\nu)/BR(W \to q\bar{q})$.

We obtain the results with a maximum likelihood to combine all Information. The b is measured to be 0.99 ± 0.29 and $b > 0.58$ at 95% confidence level. In a three-generation standard model,

$$b = \frac{|V_{tb}|^2}{|V_{td}|^2 + |V_{ts}|^2 + |V_{tb}|^2}.$$

Assuming three-generation unitarity this yields that $|V_{tb}| = 0.99 \pm 0.15$ and $|V_{tb}| > 0.76$ at 95% confidence level.

3.5 Search for Rare Decays

Within the standard model, Flavor Changing Neutral Current(FCNC) decays of a top quark are suppressed at the level of 10^{-10} to 10^{-12}. Any appearances of FCNC decays would signal the appearance of physics beyond the standard model.

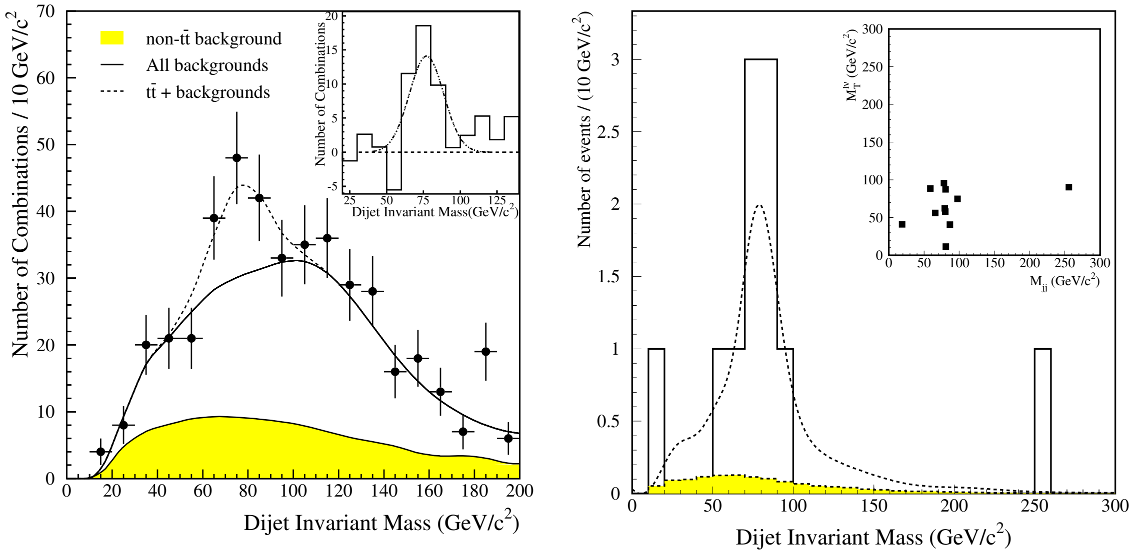

Figure 3: The dijet mass distributions for pretagged W + 4-jet events after $H_T > 310 GeV$ cut (Left) and for double b-tagged W + 4-jet events (Right) together with a fitted curve. VECBOS W + jets background is shown by a shaded curve. A sum of HERWIG $t\bar{t}$ with a top quark mass of 175 GeV/c^2 and the background is shown by a dotted curve.

We search $t\bar{t}$ events with one top decaying in the standard fashion ($t \to Wb$) and the other top quark decaying to a rare mode [18]:

- $t \to \gamma\ c, \quad t \to \gamma\ u$ (BR $\approx 10^{-10}$)
- $t \to Zc$

We search for $t \to \gamma\ q$ in the γ+4 jets and γ+lepton+jet+$\not{E}_T$ channels. We obtain the branching ratio limit:

$$BR(t \to c\gamma) \quad + \quad BR(t \to u\gamma) \quad < \quad 2.9\% \quad (95\% C.L.).$$

We search for $t \to Zq$ assuming Z decays leptonically and t decays hadronically. The search yields:

$$BR(t \to Zu) \quad + \quad BR(t \to Zc) \quad < \quad 33\% \quad (95\% C.L.).$$

4 B Physics

4.1 Hadron Lifetime Measurements

There is a question about the decay mechanism of heavy flavor mesons whether the heavy quark in a meson decays alone, or the other quark is an essential part of the process. About charm mesons, $\tau(D^+)/\tau(D^0)$ is about 2.5 because a non-spectator diagram has significant contribution. In the case of bottom mesons higher b mass makes a spectator diagram dominates and theoretical prediction yields that $\tau(B^+)/\tau(B^0)$ is about 1.05. We utilize the following decay modes for B-hadron lifetime measurement: fully reconstructed decays $B \to J/\Psi K$ and partially reconstructed decays $B \to D\ell\nu X$.

In fully reconstructed decays $B \to J/\Psi K$, we have a clean signal peak in the distribution of $J/\Psi K$ invariant mass as shown in Fig. 4. We perform the lifetime measurement with $B \to J/\Psi K$ signal sample [19]. Though this sample includes the background, the proper decay length distribution for this background is determined from the sideband sample outside of the B peak region in this mass distribution. The two sideband regions have each 60 MeV/c^2 width and start at $\pm$60 MeV/c^2 away from the world average B-mass of 5.279 MeV/c^2 [17]. The background shape is a sum of a central Gaussian, a left side exponential and a right side exponential. The two exponentials account for any non-Gaussian tails.

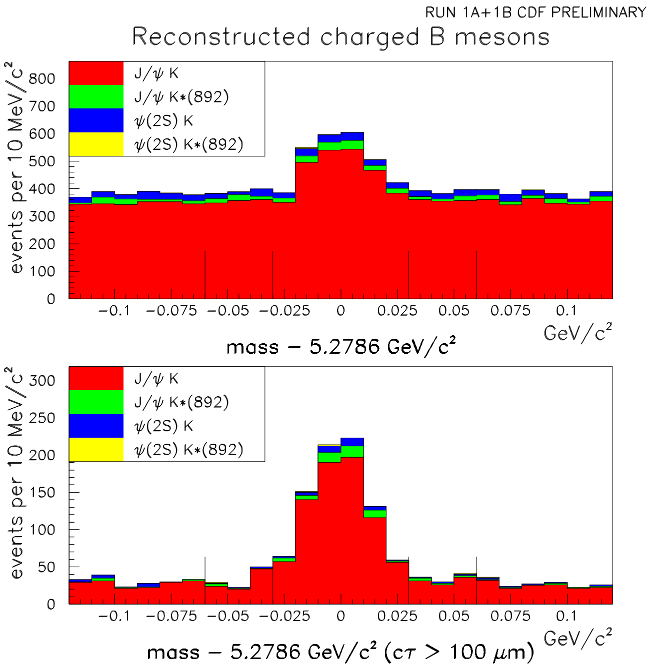

Figure 4: The $J/\Psi K$ invariant mass for charged B mesons.

Then the proper decay length distribution for the signal sample is fitted to a sum of the $B \to J/\Psi K$ signal shape (an exponential convoluted with a Gaussian resolution function) and the background shape as shown in Fig. 5. We measure the lifetime of B mesons to be 1.68±0.07(stat)±0.02(syst) ps for $B^{\pm}$ mesons and 1.58±0.09(stat)±0.02(syst) ps for B^0 mesons, and the lifetime ratio $\tau(B^+)/\tau(B^0)$ to be 1.06±0.07(stat)±0.02(syst).

In partially reconstructed decays $B \to D\ell\nu X$, we use the following four modes:

(a) $D^0 \to K^-\pi^+$ (non-D^{*+})

(b) $D^{*+} \to D^0\pi^+, D^0 \to K^-\pi^+$

(c) $D^{*+} \to D^0\pi^+, D^0 \to K^-\pi^+\pi^+\pi^-$

(d) $D^{*+} \to D^0\pi^+, D^0 \to K^-\pi^+\pi^0$

The distributions of the D meson mass or the mass difference between D and D^* mesons have a clean peak for the signal as shown in Fig. 6. The pseudo-proper decay length distributions are fitted to a sum of the B signal shape and the background shape as shown in Fig. 7. We measure the lifetime of B mesons to be 1.64±0.06(stat)±0.05(syst) ps for $B^{\pm}$ mesons and 1.48±0.04(stat)±0.05(syst) ps for B^0 mesons, and the lifetime ratio $\tau(B^+)/\tau(B^0)$ to be 1.11±0.06(stat)±0.03(syst).

4.2 $B^0 - \bar{B}^0$ Mixing

B^0 and $\bar{B}^0$ are distinct to strong interaction and mix via the weak interaction. The free propagation and decay eigenstates are

$$|B_L\rangle = \frac{1}{\sqrt{2}}\left[|B^0\rangle - |\bar{B}^0\rangle\right]$$
$$|B_H\rangle = \frac{1}{\sqrt{2}}\left[|B^0\rangle + |\bar{B}^0\rangle\right]$$

with masses m_L and m_H. Our goal is to measure $\Delta m = m_H - m_L$ which yields $|V_{td}|$ and $|V_{ts}|$.

A produced B^0 is initially $\Psi(0) = \frac{1}{\sqrt{2}}\left[|B_L\rangle + |B_H\rangle\right]$. With time, B_L and B_H components develop the relative phase and make a non-zero $\bar{B}^0$ component:

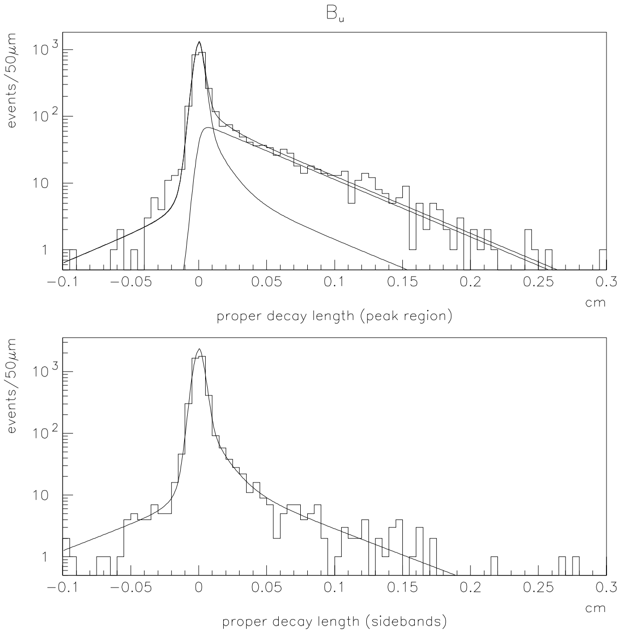

Figure 5: The lifetime distribution for $J/\Psi K$ for charged B mesons.

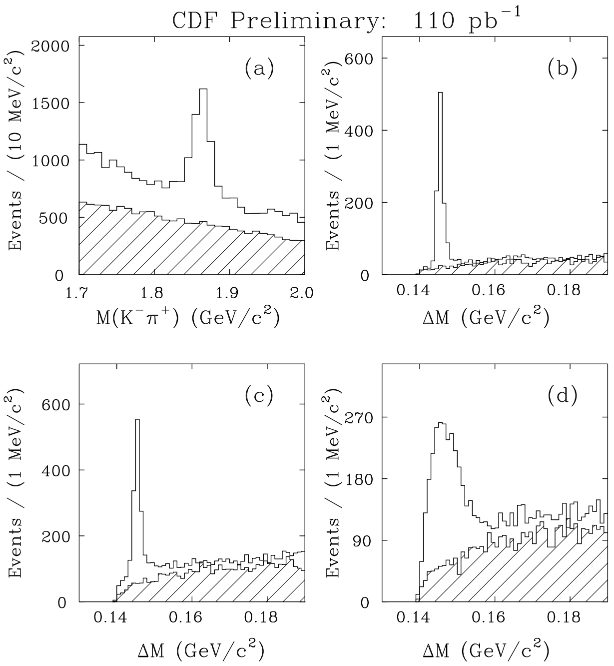

Figure 6: The distributions of the D meson mass for (a) and the mass difference between D and D^* mesons for (b) through (d). Shaded histograms correspond to wrong sign combination.

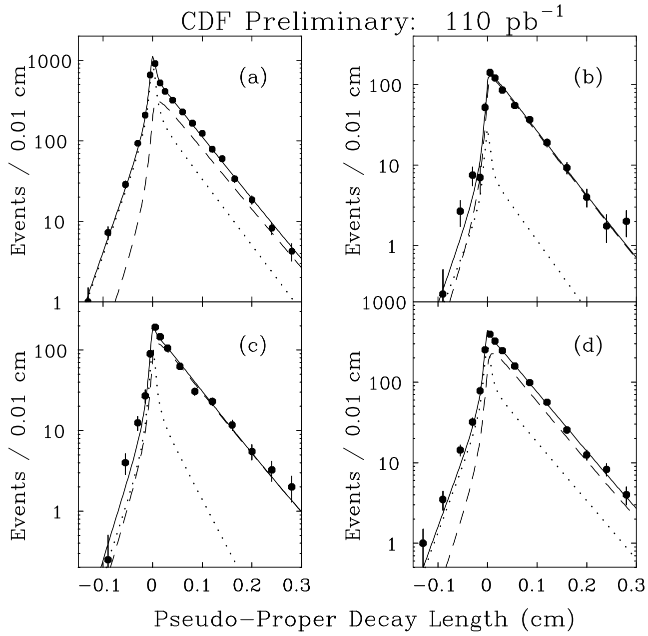

Figure 7: The lifetime distribution for $B \to D\ell\nu X$.

$P(t)_{B^0\to B^0} = \frac{1}{2\tau}e^{-\frac{t}{\tau}}(1 + cos\Delta mt)$: unmixed probability,
$P(t)_{B^0\to \bar{B}^0} = \frac{1}{2\tau}e^{-\frac{t}{\tau}}(1 - cos\Delta mt)$: mixed probability,
where τ is a lifetime and t is a proper time.

To extract Δmt, we measure the asymmetry defined by

$$A(t) \quad \equiv \quad \frac{N_{B^0\to B^0}(t) - N_{B^0\to \bar{B}^0}(t)}{N_{B^0\to B^0}(t) + N_{B^0\to \bar{B}^0}(t)} = D_0 cos\Delta mt$$

Mistags, *i.e.* incorrect flavor determinations, result in a decrease of the oscillation amplitude by the B^0 dilution factor D_0. We measure the asymmetry as a function of the proper decay length ct and fit them with their expected time dependence, obtaining Δm_d and D_0.

The decay time is measured using either ℓ^-+ inclusive "charm" vertex or ℓ^-+ exclusive D reconstruction. The former has high statistics but low $\bar{B}^0$ purity, while the latter has low statistics but high $\bar{B}^0$ purity.

We use several flavor tagging techniques such as the sign of lepton in decay ($b \to \mu^-; \bar{b} \to \mu^+$) and the momentum weighted charge of the particles in the decay, *i.e.* jet charge (b is $-$; $\bar{b}$ is $+$) on the opposite side. On the same side, we use the electric charge of particles produced near the B meson which provides a basis for Same Side Tagging (SST) [20]. For example, if a $\bar{b}$ quark combines with a u quark to form a B^+ meson, the remaining $\bar{u}$ quark may combine with a d quark to form a π^+.

We have four kinds of analyses as listed in Table 4 and obtain oscillation results as shown in Fig. 8. In the Analyses I and IV, we make a likelihood function by a product of the expected probabilities of the proper decay length for the $b\bar{b}$ same sign and opposite sign events, and perform an unbinned likelihood fit for the $b\bar{b}$ candidates events to extract Δm_d and the dilution factors. In the Analysis II, we measure the $b\bar{b}$ same sign fraction as a function of proper decay length and make a χ_2 fit to the expected time dependence, obtaining Δm_d. In the Analysis III, we measure the asymmetry A as a function of the proper decay length and make a χ^2 fit to the expected time dependence, obtaining Δm_d. Combining these four results, we measure Δm_d to be 0.464 $\pm$ 0.030(stat) $\pm$ 0.026(syst) ps^{-1}. A world average of Δm_d measurements yields including this CDF result 0.473 $\pm$ 0.011(stat) $\pm$ 0.014(syst) ps^{-1} which results in $|V_{td}| = (8.6\pm0.2(\text{stat})\pm0.2(\Delta m_{top})\pm1.7(\text{theory})) \times10^{-3}$. The updated Analysis III yields Δm_d of 0.471 $^{+0.078}_{-0.068}$(stat) $\pm$ 0.030(syst) ps^{-1} as reported in Ref. [20].

	TRIGGER	SIGNAL	TAG	STAT
I	$\ell > 8GeV$	ℓ + inc. vertex	soft-ℓ or Q(jet)	170k
II	$e, \mu > 5{,}3$	$e(\mu)$ + inc. vertex	soft-$\mu(e)$	10k
III	$\ell > 8GeV$	$\ell^- + D^{(*)+}$	"same side" pion	6000
IV	$\mu, \mu > 2{,}2$ $e, \mu > 5{,}3$	$\ell^- + D^{(*)+}$	soft-ℓ	500

Table 4: Four analyses on time-dependent $B^0 - \bar{B}^0$ mixing.

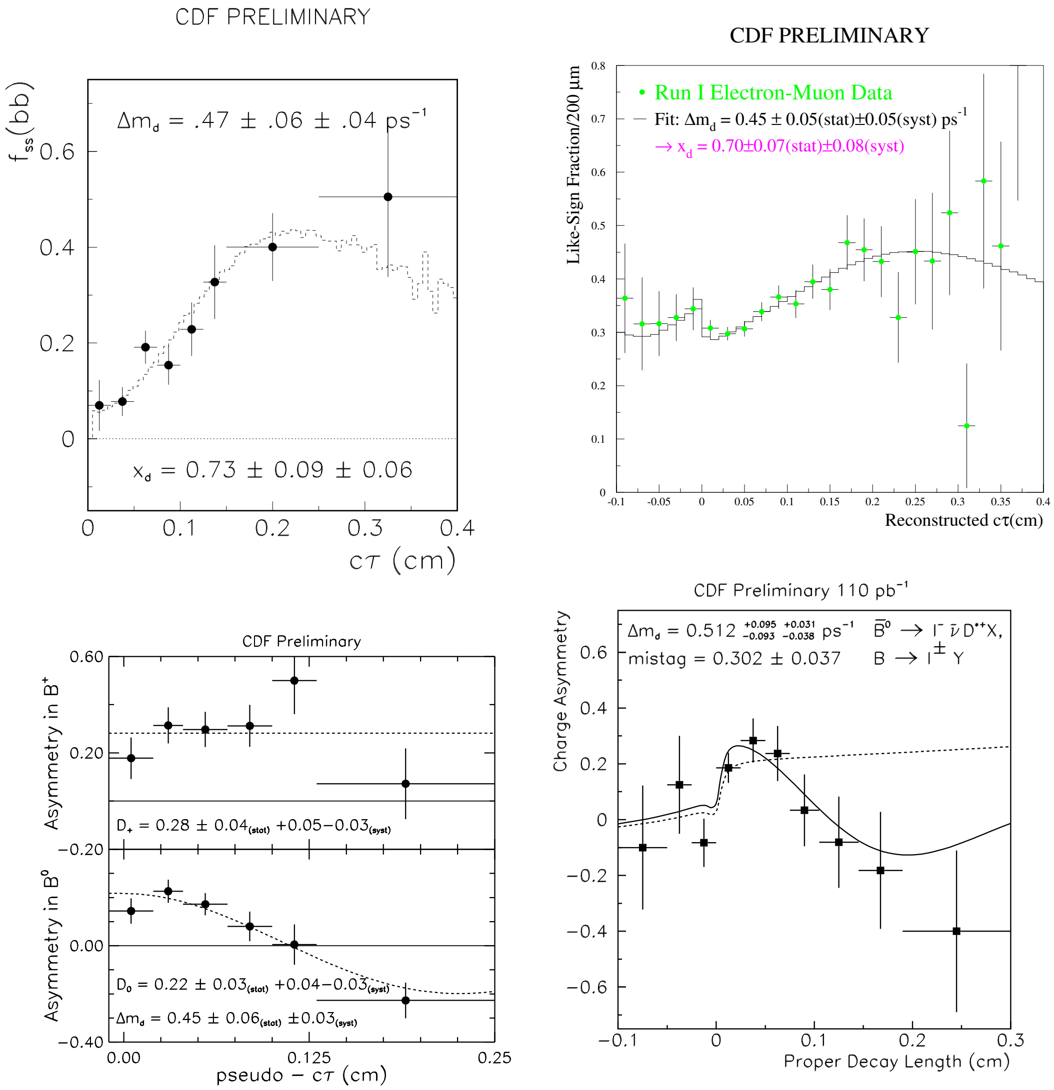

Figure 8: Time-dependent $B^0 - \bar{B}^0$ mixing for Analysis I (Top Left) with a signal of ℓ + inclusive vertex and a b-tag of soft ℓ or Jet charge, for Analysis II (Top Right) with a signal of $e(\mu)$ + inclusive vertex and a b-tag of soft $\mu(e)$, for Analysis III (Bottom Left) with a signal of $\ell^- + D^{(*)+}$ and a b-tag of same side pion, and for Analysis IV (Bottom Right) with a signal of $\ell^- + D^{(*)+}$ and a b-tag of soft ℓ.

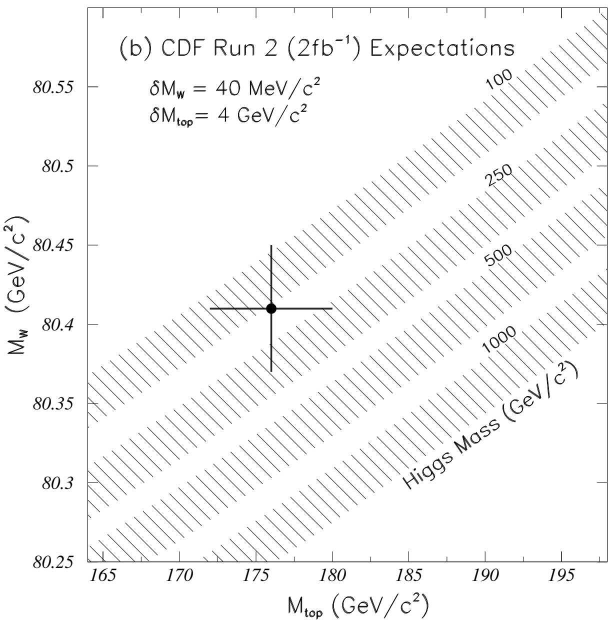

Figure 9: Accuracies on W mass and top quark mass expected in Run2 together with predicted curves at various Higgs masses.

5 Future Prospects at the Tevatron

We are upgrading the CDF detector [21] so as to work on the upgraded Tevatron collider in the next Run2 which will start in the beginning of 2000. By the accelerator upgrade, the center-of-mass energy will be increased from 1.8 TeV to 2.0 TeV ($\sigma_{t\bar{t}}$ becomes higher by a factor of 1.4) and the integrated luminosity will be increased from 0.1 fb^{-1} to 2 fb^{-1} by a factor of 20. By the detector upgrade, the acceptance for $t\bar{t} \to W(\to \ell\nu) + \geq 3$ jet events will increase from 9.5% to 12% (by a factor of 1.3) and the b-tagging efficiency for b-jets will increase from 42% to 80% (by a factor of 2). ¿From the above, we have 70 times higher rate of $t\bar{t} \to W(\to \ell\nu) + \geq 3$ jet events with one b-tagged jet in Run2. In Run2, we expect $t\bar{t}$ events such as 1,200 $W(\to \ell\nu) + \geq 4$ jet events with one b-tagged jet, and 600 $W(\to \ell\nu) + \geq 4$ jet events with two b-tagged jets.

5.1 Top Quark Physics in Run2

We will measure the top quark mass with an uncertainty $\Delta M_{top} < 4GeV/c^2$ which will yield a tighter constraint to a Higgs mass together with a new W mass as shown in Fig. 9. We will also measure the $t\bar{t}$ production cross section with $\Delta\sigma/\sigma \sim 7\%$ and the top quark decay width Γ_{top} from $q\bar{q} \to W^* \to t\bar{b}$. We will search for new particles such as $X \to t\bar{t}$ where X is a color octet vector meson, Z' or something else.

5.2 B physics in Run2

To find the CP violation in B meson system, we need observe the unequal number of $B^0 \to J/\Psi K_s$ and $\bar{B}^0 \to J/\Psi K_s$. In Run2, we will have $10,000 \sim 15,000$ $J/\Psi K_s$ events with $\epsilon_{eff} = 4 \sim 8$ % which enables us to measure $\sin 2\beta$ with $\delta \sin 2\beta = 0.08 \sim 0.14$ while the theoretical prediction of $\sin 2\beta$ is between 0.2 and 0.8. ϵ_{eff} is an effective tagging efficiency given by ϵD_0^2 where ϵ is a flavor tagging efficiency and D_0 is the dilution factor. Another CP violation causes the unequal number of $B^0 \to \pi^+\pi^-$ and $\bar{B}^0 \to \pi^+\pi^-$. To observe this is much harder because it is hard to trigger on with SVT and has

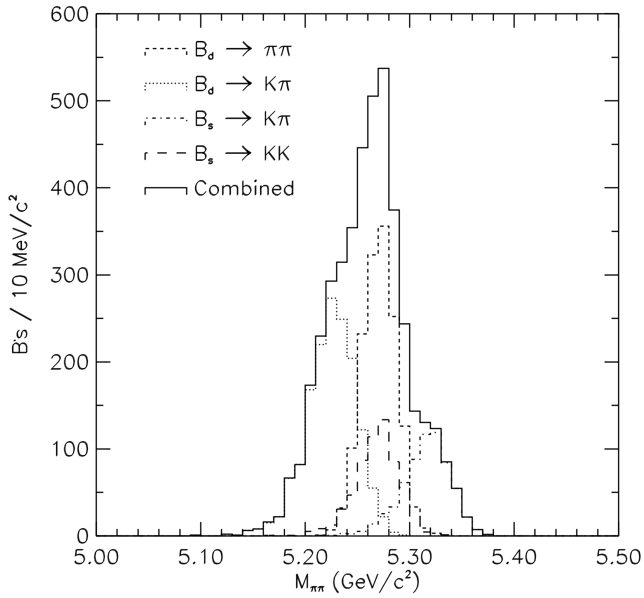

Figure 10: Invariant mass distributions of two charged tracks which were assumed to be pions.

more difficult backgrounds than the first one as shown in Fig. 10. The SVT is a trigger which detects the presence of tracks with displaced vertices using the SVX. dE/dX measurement will be helpful for the separation of $B^0 \to \pi^+\pi^-$ from the backgrounds. In Run2, we expect about 10,000 $B^0 \to \pi^+\pi^-$ events and $\delta \sin 2\alpha$ around 0.10.

On the $B_s^0 - \bar{B}_s^0$ mixing we need the b-tagging capability and the good proper-time resolution. The oscillation length for $B_s^0 - \bar{B}_s^0$ mixing is much shorter than for $B_d^0 - \bar{B}_d^0$ mixing. Assuming $x_s = 20$ ($x_s = \Delta m_s/\Gamma(B_s)$), we will have a plot of a mixed fraction against a proper decay length as shown in Fig. 11 for $B_s^0 \to D_s{+}n\pi$ decays of about 2,000 tagged events in Run2. Thus we will be able to observe this oscillation for $x_s = 20$. We have the sensitivity over full range of oscillation length using both the partially reconstructed decays $B_s \to D_s \ell \nu X$ and the fully reconstructed decays $B_s \to J/\Psi\phi$. The difference between $\tau(B_s^H)$ and $\tau(B_s^L)$ yields $\Delta\Gamma(B_s)$. It yields Δm_s together with a theoretical calculation of $\Delta\Gamma(B_s)/\Delta m_s$.

6 Summary

Top quark production has been observed and the $t\bar{t}$ production cross section was measured in the dilepton, lepton+jets and all-hadronic channels. The combined $t\bar{t}$ production cross section between the three channels is $7.6^{+1.8}_{-1.5}$ pb. The new results of top quark mass is obtained with the optimal use of information. The top quark mass is 175.9±6.9 GeV/c^2. Nothing observed in top production and decay is inconsistent with the standard model. In the next run of the Fermilab Collider, we will measure the top quark mass more accurately which yields a more stringent Higgs mass limit together with a new W mass.

Basic techniques for detailed B studies have been successfully carried out with the CDF detector. CDF is producing many high quality B physics measurements. There is much to be learned about CP violation in $B - \bar{B}$ system in the next run of the Fermilab Collider.

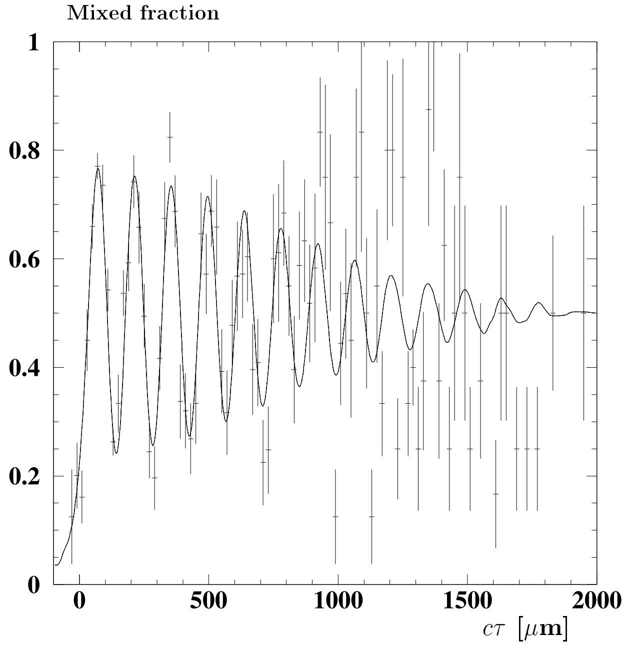

Figure 11: A plot of a mixed fraction against a proper decay length assuming $x_s = 20$.

Acknowledgements

I would like to thank the organizers of this conference for their warmth and hospitality. I also wish to thank all the people who made this conference a special place. The works presented here represent the efforts of all the members of the CDF collaboration.

References

[1] S. W. Herb *et al.*, Phys. Rev. Lett., **39**, 252 (1977).

[2] F. Abe *et al.*, (The CDF collaboration) Phys. Rev. Lett. **73**, 225 (1994);
F. Abe *et al.*, (The CDF collaboration) Phys. Rev. D**50**, 2966 (1994).

[3] F. Abe *et al.*, (The CDF collaboration) Phys. Rev. Lett. **74**, 2626 (1995).

[4] F. Abachi *et al.*, (The D0 collaboration) Phys. Rev. Lett. **74**, 2632 (1995).

[5] F. Abe *et al.*, Nucl. Instrum. Methods Phys. Res., Sect. **A 271**, 387 (1988).

[6] S. Cihangir *et al.*, Nucl. Instrum. Methods Phys. Res., Sect. **A 360**, 137 (1995). Our previous silicon vertex detector is described in D. Amidei *et al.*, Nucl. Instrum. Methods Phys. Res., Sect. **A 350**, 73 (1994).

[7] In the CDF coordinate system, θ is the polar angle with respect to the proton beam direction. The pseudorapidity η is defined as $-\ln\tan(\theta/2)$. The transverse momentum of a particle is $P_T = P\sin\theta$. The analogous quantity using calorimeter energies, $E_T = E\sin\theta$, is called transverse energy. Missing transverse energy $\not{E}_{\rm T}$ is defined as $-\Sigma E_T^i \cdot \hat{n}_i$, where $\hat{n}_i$ are the unit vectors, in the plane transverse to the beam line, pointing from the interaction point to the energy deposition in cell i of the calorimeter.

[8] F. Abe *et al.*, FERMILAB-PUB-97/286-E. submitted to Phys. Rev. Lett.

[9] Laenen, Smith & van Neerven, Phys. Lett. **B321** 254 (1994);
Berger & Contopanagos, Phys. Rev. **D54** 3085 (1996);
S. Catani, M.L. Mangano, P. Nason, & L. Trentadue, Phys. Lett. **B378** 329 (1996).

[10] G. Marchesini and B. R. Webber, Nucl. Phys. **B 310**, 461 (1988);
G. Marchesini *et al.*, Comput. Phys. Comm. **67**, 465 (1992).

[11] F. A. Berends, W. T. Giele, H. Kuif, B. Tausk, Nucl. Phys. **B 357**, 32 (1991);
W. Giele, Ph. D. Thesis, Leiden (1989).

[12] F. Abe *et al.*, FERMILAB-PUB-97/304-E. submitted to Phys. Rev. Lett.

[13] F. Abe *et al.*, FERMILAB-PUB-97/075-E. submitted to Phys. Rev. Lett.

[14] F. Abe *et al.*, FERMILAB-PUB-97/284-E. submitted to Phys. Rev. Lett.

[15] LEP electroweak working group, 1997 Lepton Photon conference.

[16] F. Abe *et al.*, FERMILAB-PUB-97/285-E. submitted to Phys. Rev. Lett.

[17] Particle Data Group, Phys. Rev. **D54** (1996).

[18] F. Abe *et al.*, FERMILAB-PUB-97/270-E. submitted to Phys. Rev. Lett.

[19] F. Abe *et al.*, FERMILAB-PUB-97/352-E. submitted to Phys. Rev. D.

[20] F. Abe *et al.*, FERMILAB-PUB-97/312-E. submitted to Phys. Rev. Lett.

[21] The CDF II Collaboration, FERMILAB-PUB-96/390-E (1996).